

## Engineering of Ultraviolet reflectors by varying alternate layers of Titania/Silica for harmful UV-protection

R.S. Dubey

*Advanced Research Laboratory for Nanomaterials and Devices,  
Dept. of Nanotechnology, Swarnandhra College of Engineering and Technology,  
Narsapur (A.P.), Seetharampuram, India  
Corresponding author: rag\_pcw@yahoo.co.in*

### Abstract

This paper presents the engineering of ultraviolet (UV) reflectors made up of alternate layers of titania ( $\text{TiO}_2$ ) and silica ( $\text{SiO}_2$ ) by using the sol-gel spin coating method. The choice of these two materials is appropriate to realize the optical reflectors due to their large refractive index contrast. The formation of multilayer films of  $\text{TiO}_2$  and  $\text{SiO}_2$  are studied by field emission scanning electron microscopy (FESEM), while UV-vis spectroscopy measurement is performed to study the reflectance. By varying the number of  $\text{TiO}_2/\text{SiO}_2$  stacks, we have achieved the maximum reflectance within the UV region at center wavelengths of 335 nm, 358 nm, and 367 nm corresponding to the 3-, 6-, and 9-stacks based reflectors. Finally, it is summarized that these reflectors prohibit the propagation of ultraviolet light, and therefore, promising for UV protection coating.

**Keywords:** Cross-section morphology; reflection; reflectors; thin films; UV Reflector.

### 1. Introduction

The solar spectrum is composed of ultraviolet (UV), visible (Vis), and infrared (IR) radiations. Out of these, UV radiation has adverse effects on human life, which causes sunburn, immune system, suntan, DNA damage, and ageing. Furthermore, UV exposure damages the human body, which often induces darker skin and macular degeneration in the eyes (Chalam *et al.*, 2021). It is, therefore, rather essential that human bodies are protected and safe from exposure to ultraviolet radiation. Reflectors are merely passive devices created by metal and dielectric layers. Nonetheless, due to their high maintenance and manufacturing costs, metal reflectors are of low interest. Thus, dielectric reflectors are the alternative to conventional metal reflectors and can be tailored for the interesting wavelength region. Such reflectors can be made by preparing alternate films of two different dielectric materials: zinc oxide, zirconium dioxide, hafnium dioxide, silicon dioxide, aluminum oxide, and titanium dioxide. The refractive index contrast of the corresponding materials is the primary consideration in manufacturing dielectric reflectors. The greater the refractive index contrast, the higher will be the reflectance window (Flannery *et al.*, 1979). Among the above-discussed dielectric materials, the combination of  $\text{TiO}_2/\text{SiO}_2$  materials with their refractive index contrast 2.4/1.4 is the best choice for fabricating dielectric reflectors. Such reflectors can be produced using chemical vapor deposition, physical vapor deposition, angles of glancing, sol-gel-spin-coating, dip-coating, and spray pyrolysis methods (Jung *et al.*, 2008; Kitano *et al.*, 2006; Singh *et al.*, 2015; Vincent *et al.*, 2007; Yuehui *et al.*, 2018; Abou-Helal *et al.*, 2002). One should carefully choose a suitable method for fabricating such dielectric reflectors to minimize the

production cost and the processing time. The sol-gel spin coating process is beneficial over other techniques due to its simple and easy control of process parameters (Subramanian *et al.*, 2008; Wu *et al.*, 2001; Zhang *et al.*, 2012). These reflectors can be adopted as a UV coating material for the glass windows of houses/buildings/offices for UV protection to human skin and the eyes. It is also beneficial to resist ultraviolet radiation during the biological process for protecting useful bacteria. These multilayer dielectric structures have other applications, such as complimentary metal-oxide-semiconductor (CMOS) devices, flame sensors, space communications, and rocket systems (Monroy *et al.*, 2003; Yonemaru *et al.*, 2002; Xie *et al.*, 2007). Various research groups have reported the fabrication and realization of UV reflectors. Plasma-CVD fabrication of  $\text{SiO}_2/\text{Si}_3\text{N}_4$  reflector having 27 layers of  $\text{SiO}_2$  and  $\text{Si}_3\text{N}_4$  demonstrated maximum reflectance in the UV wavelength range (Dai *et al.*, 2016). The preparation of dense multilayer reflectors based on  $\text{HfO}_2/\text{SiO}_2$  films using the plasma-ion-assisted technique was reported to deal with ultraviolet light. The reflector based on 23 layers of  $\text{HfO}_2/\text{SiO}_2$  endorsed the reflectance window in the ultraviolet region with the minimum optical loss (Torchio *et al.*, 2002). A report on the fabrication of a 22-layer-based ultraviolet reflector using the ion-assisted e-beam evaporation method is presented. They explored the performance of light-emitting diodes integrated with UV reflectors and showed better performance (Lin *et al.*, 2015). An ultraviolet reflector composed of 26 layers of  $\text{LaF}_3$  and  $\text{MgF}_2$  prepared by thermal evaporation technique was employed for the far-ultraviolet radiation. They explored the application of fabricated reflectors for the wide-angle aurora imager (Wang *et al.*, 2018). Various multilayer structures based on 99, 55 and 35 layers of  $\text{BaF}_2$  and  $\text{LaF}_3$  fabricated by the e-beam evaporation technique were studied. The reflectance of these UV reflectors was noticed to be 96.5 %, 95.3 %, and 93.6 % based on samples 99-, 55- and 35-layers (Zukic *et al.*, 1991). Further, a dielectric reflector composed of 25 layers of  $\text{LaF}_3$  and  $\text{MgF}_2$  materials processed by the e-beam evaporation technique was explored. The author noticed an excellent optical property of the UV reflector and suggested its application in the Fabry-Perot interferometer (Malherbe *et al.*, 1974). Similarly, another group reported the preparation of an 8-layer based dielectric mirror composed of  $\text{Al}/\text{MgF}_2$  films by using the electron-beam evaporation technique. This prepared structure endorsed the reflection of the UV-A spectrum. This experimental finding was compared with the simulated result and found in good agreement. Further, they suggested the application of the reflector in the Fabry-Perot interferometer (Spiller *et al.*, 174). A multilayer thin-film structure based on seven stacks of  $\text{TiO}_2/\text{SiO}_2$  was fabricated by adopting the sol-gel spin coating technique. The prepared reflector is endorsed as much as 100% reflectance in the UV spectrum (Dubey *et al.*, 2017).

According to the above-reported literature, we have noticed that fabricated reflectors comprise many layers, which severely affects the fabrication cost and processing time of such reflectors. So, the development of low-cost reflectors is essential to save resources. In this paper, we report the engineering of UV reflectors by varying the number of  $\text{TiO}_2$  and  $\text{SiO}_2$  layers with the projection to reduce the fabrication cost and processing time. Section 2 presents the experimental approach, and the results are explored in section 3. Section 4 summarizes the work.

## 2. Experimental approach

The chemicals used in the synthesis process of  $\text{TiO}_2/\text{SiO}_2$  gels do not require any extra further

purification. Tetra-butylorthotitanate (TBOT) and tetraethyl orthosilicate (TEOS) procured from Sigma-Aldrich were used as the precursors for fabricating the  $\text{TiO}_2$  and  $\text{SiO}_2$  thin films. For gel preparation, solvent 'ethanol' and catalyst 'acetic acid' was preferred. The gel of  $\text{TiO}_2$  was synthesized using TBOT, ethanol, and acetic acid in the molar ratio of 1.2:20:1.7, respectively. Ethyl alcohol and acetic acid were thoroughly mixed under continuous magnetic stirring for 15 minutes. Later, precursor TBOT was added drop-by-drop under vigorous stirring. Further, stirring was maintained for a period of 3 hr. The asobtained  $\text{TiO}_2$  gel was clear and transparent, which was left for 24 hr ageing. Similarly,  $\text{SiO}_2$  gel was synthesized using TEOS, ethanol and, acetic acid in the molar ratio of 1.5:20:2.3, respectively. The gel was synthesized by slowly adding the precursor TEOS solution in the ethanol and acetic acid mixed solution under continuous stirring. The stirring process was continued for 4 hr to obtain a transparent gel. Finally, the solution was left for 24 hr ageing. After ageing, the solutions were found viscous enough and used for the film preparation on the cleaned glass substrates. The spin rate and spin duration were fixed to 2500 RPM for 30 sec. Multilayer structures of  $\text{TiO}_2/\text{SiO}_2$  were deposited alternately by spin coating. After fabrication, each film of  $\text{TiO}_2$  and  $\text{SiO}_2$  was sintered at temperatures of 500 °C and 300 °C, respectively, for about 60 min. The spin coating process was repeated to fabricate the dielectric reflectors based on three, six, and nine alternate films. The fabricated multilayer structures were examined for surface and cross-section morphology using field-emission scanning electron microscopy (FESEM, ZEISS, Germany). The elements composition investigation was performed using energy-dispersive x-ray spectroscopy (EDS) attached to FESEM. The reflectance analyses were carried out using an ultraviolet-visible spectrophotometer (UV-vis, UV1800 Shimadzu, Japan).

### 3. Results and discussion

We have performed the FESEM measurement to analyze the surface and cross-section morphology. Figure 1 depicts the top-view and cross-sectional FESEM images, EDS, and reflectance spectra of three stack-based reflectors of  $\text{TiO}_2/\text{SiO}_2$  thin films. Figure 1(a) and 1(b) show the top view of 3-stacks based  $\text{TiO}_2/\text{SiO}_2$  reflector recorded at 1  $\mu\text{m}$  and 100 nm scale, respectively. We can observe the uniform coating of the top  $\text{TiO}_2$  film. The average grain size of the top  $\text{TiO}_2$  film was estimated to be 7.5 nm. The cross-section view of the reflector is shown in Figures 1(c) and 1(d) recorded at a scale of 1  $\mu\text{m}$  and 200 nm, respectively. We can observe the formation of a multilayer structure consisting of periodically arranged  $\text{TiO}_2/\text{SiO}_2/\text{TiO}_2/\text{SiO}_2/\text{TiO}_2/\text{SiO}_2$  films having thicknesses of 37.05 nm, 55.42 nm, 22.12 nm, 66.46 nm, 37.05 nm, and 103.5 nm, respectively in figure 1(d) recorded at a scale of 200 nm. EDS spectroscopy was performed to know the elemental composition in the multilayer structures. Figure 1(e) shows the presence of Ti, O, and Si peaks at 0.45keV, 0.5keV, and 1.7 keV, respectively. Reflectance spectra of 3-stacks-based  $\text{SiO}_2/\text{TiO}_2$  reflector is plotted in the wavelength range from 300-400 nm, as shown in figure 1(f). The opening of a reflection band can be noticed with its reflectance of 76 % at the center wavelength of 335 nm. Further, we have engineered the reflector's fabrication to maximize the reflectance in a broad range of UV spectrum. With this, we have fabricated a 6-stacks-based  $\text{TiO}_2/\text{SiO}_2$  reflector, as shown in figure 2. Compared to 3-stacks based  $\text{TiO}_2/\text{SiO}_2$  reflector, uniform deposition of the films can be noticed as depicted in figure 2(a). FESEM image recorded at an increased scale as shown

in figure 2(b), which depicts similar grains with an average diameter of 6.5 nm. We can observe the layered structure of  $\text{TiO}_2$  and  $\text{SiO}_2$  in the cross-section FESEM image recorded at a scale of  $1\ \mu\text{m}$ , as shown in figure 2(c). In contrast, a closer look at the 6-stacks-based  $\text{TiO}_2/\text{SiO}_2$  reflector shows distinct layers of  $\text{TiO}_2$  and  $\text{SiO}_2$  with slightly different morphology of individual layers.

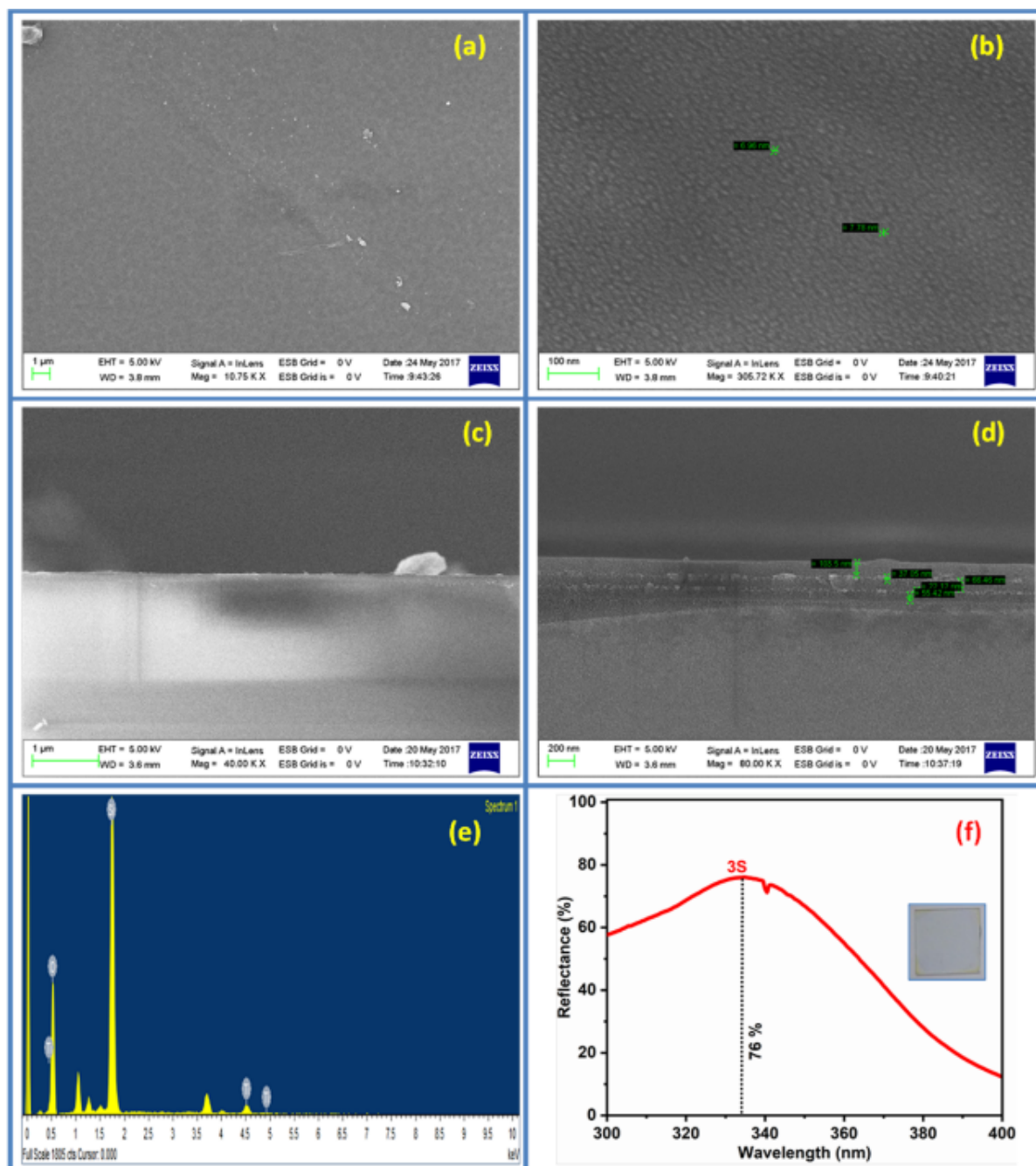


**Fig. 1.** FESEM top-view fig.(a)-fig.(b) recorded at the scale of  $1\ \mu\text{m}$  and  $100\ \text{nm}$ , a cross-sectional view fig.(c)-fig.(d) recorded at the scale of  $1\ \mu\text{m}$  and  $200\ \text{nm}$ , EDS spectra fig.(e) and reflectance spectra fig.(f) of 3-stacks  $\text{TiO}_2/\text{SiO}_2$  reflector.

The calculated thicknesses of each  $\text{TiO}_2/\text{SiO}_2$  film were  $22/75.22$ ,  $19.17/75.22$ ,  $22.21/75.57$ ,  $35/82.63$ ,  $32.47/101.8$ , and  $33.95/112.1\ \text{nm}$ , respectively. As shown in figure 2e, EDS spectra show the peaks of Ti, O, and Si elements at energy  $0.45\ \text{keV}$ ,  $0.5\ \text{keV}$ , and  $1.7$

keV, respectively. It is interesting to notice the reflectance spectra of 6-stacks-based  $\text{TiO}_2/\text{SiO}_2$  reflectors compared to 3-stacks-based reflectors, as depicted in figure 2(f). By increasing the number of stacks, one can notice an enhancement in reflectance to 100 %. Further, we can also realize the broadening and shifting of the reflection band within the range of the UV spectrum. The center wavelength is noticed to be shifted to 358 nm instead of 335 nm for the case of 3-stacks based reflector, as observed previously and also found to coincide with the reported literature (Venkatesh *et al.*, 2020).

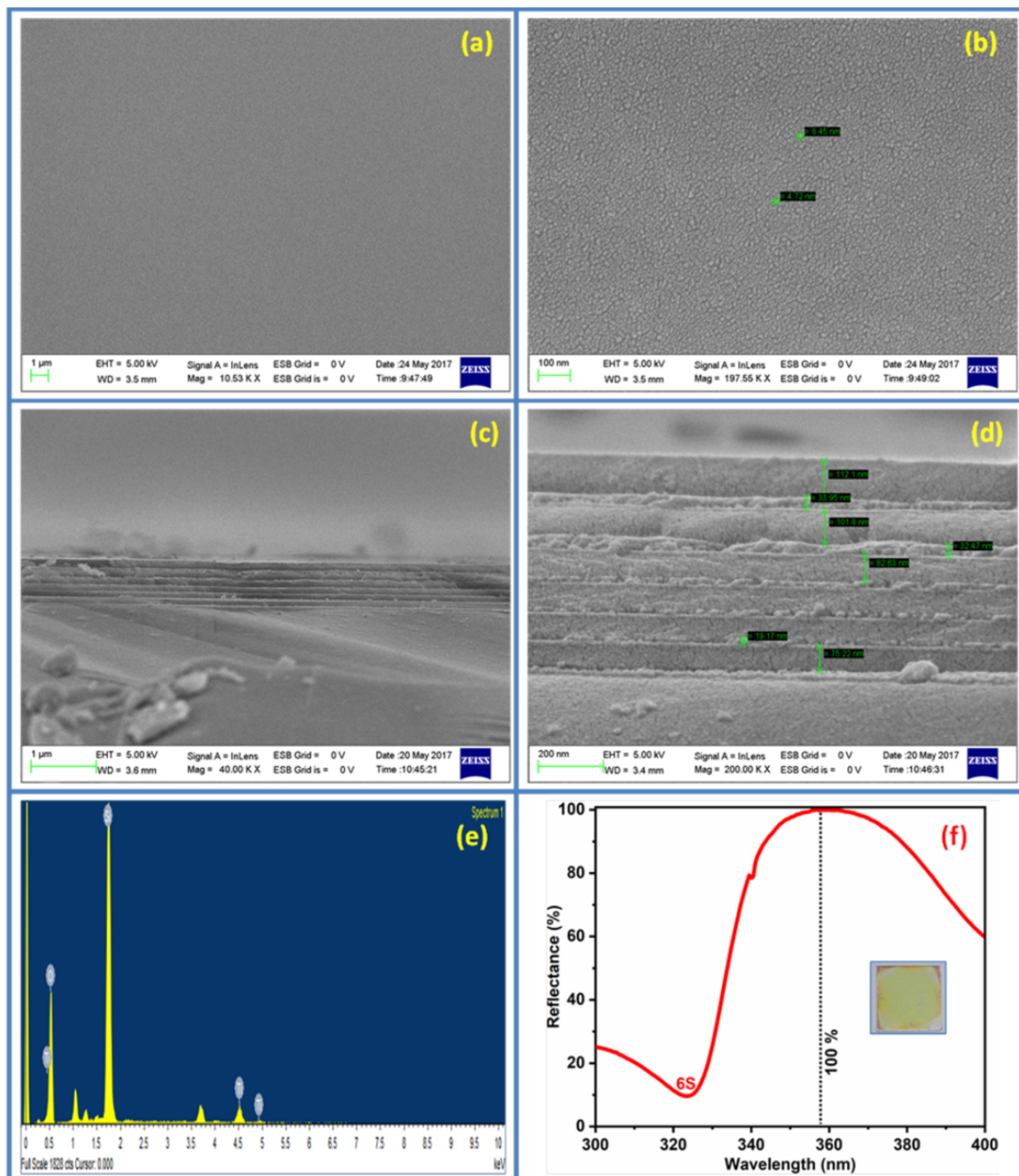


**Fig. 2.** FESEM top-view fig.(a)-fig.(b) recorded at the scale of 1  $\mu\text{m}$  and 100 nm, a cross-sectional view fig.(c)-fig.(d) recorded at the scale of 1  $\mu\text{m}$  and 200 nm, EDS spectra fig.(e) and reflectance spectra fig.(f) of 6-stacks  $\text{TiO}_2/\text{SiO}_2$  reflector.

It is interesting to notice the reflectance spectra of 6-stacks-based  $\text{TiO}_2/\text{SiO}_2$  reflectors compared to 3-stacks-based reflectors, as depicted in figure 2(f). By increasing the number of stacks, one can notice an enhancement in reflectance to 100 %. Further, we can also realize the broadening and shifting of the reflection band within the range of the UV spectrum. The center wavelength is noticed to be shifted to 358 nm instead of 335 nm for the case of 3 stacks based reflector, as observed previously and also found to coincide with the reported literature (Venkatesh et al., 2020).

Finally, we have increased the number of stacks to 9, and the obtained results are shown in figure 3. The uniform deposition of the films is noticed as visible in figure 3(a), while figure 3(b) depicts the distribution of uniform grains with their average size of 4.5 nm.

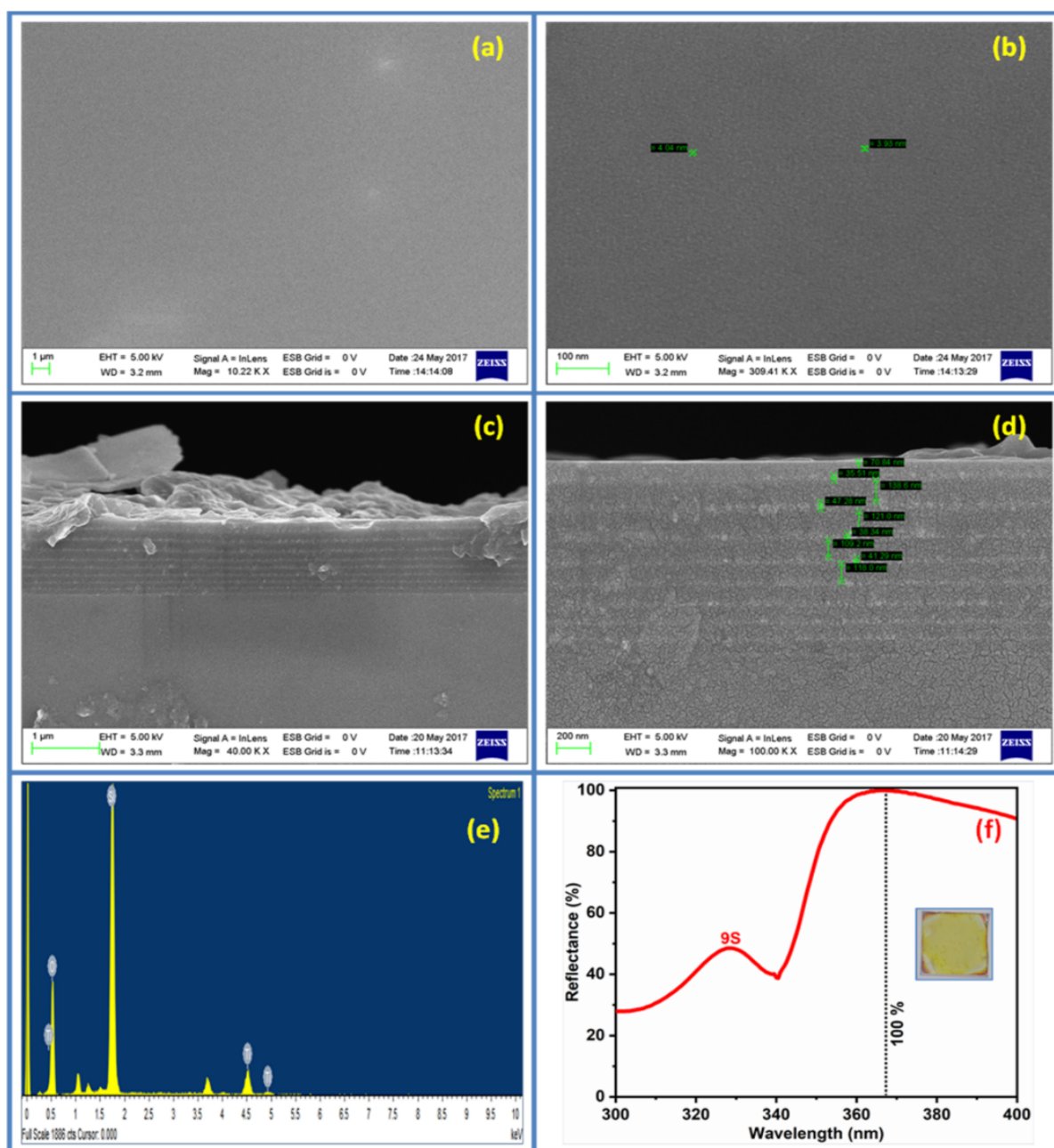


**Fig. 3.** FESEM top-view fig.(a)-fig.(b) recorded at the scale of 1  $\mu\text{m}$  and 100 nm, a cross-sectional view fig.(c)-fig.(d) recorded at the scale of 1  $\mu\text{m}$  and 200 nm, EDS spectra fig.(e) and reflectance spectra fig.(f) of 9-stacks  $\text{TiO}_2/\text{SiO}_2$  reflector.

A cross-sectional multilayer structure view can be seen in figure 3(c), while figure 3(d) depicts the 18 layers of TiO<sub>2</sub>/SiO<sub>2</sub>. The thicknesses of 18 layers of TiO<sub>2</sub>/SiO<sub>2</sub> films were 35.51/120, 47/100, 41/121, 41/118, 35/118, 41.29/ 109.2, 38.34/121, 47.26/138.6, and 35.51/70.84, respectively. The EDS spectrum is plotted in figure 3e, which shows the elemental composition of Ti, O, and Si at energy 0.45 keV, 0.5 keV, and 1.7 keV, respectively. A broader reflection window is observed for the case of a 9-stacks-based TiO<sub>2</sub>/SiO<sub>2</sub> reflector, as depicted in figure 3(f). One can notice as much as 100% reflectance at the center wavelength of 367 nm. In addition, we can observe the presence of a small reflectance peak at a wavelength of 330 nm, which could be regarded as the interference of light due to the increased number of stacks compared to previous reflectors based on 3- and 6-stacks based. With the fabrication of TiO<sub>2</sub>/SiO<sub>2</sub> reflectors by varying the number of stacks 3, 6, and 9 and one can observe corresponding shifting of their center wavelengths towards the higher values i.e., 335 nm, 358 nm, and 367 nm, and found in good agreement with the reported literature (Yuehui *et al.*, 2018). Notably, the 6 and 9-stacks-based reflectors evidence their 100 % reflectance with a broad reflection window.

#### 4. Conclusions

Using the sol-gel spin coating approach, various dielectric reflectors by varying the number of TiO<sub>2</sub>/SiO<sub>2</sub> stacks were fabricated and studied. The surface morphology investigation of 3-, 6- and 9-stacks-based reflectors evidenced the deposition of uniform films. The FESEM cross section study demonstrated the fabrication of 6, 12, and 18 periodic layers of TiO<sub>2</sub> and SiO<sub>2</sub>. The EDS spectrum confirmed the presence of elemental peaks of Ti, Si, and O in all three samples. The obtained reflectance values are 76 %, 100 %, and 100% corresponding to the TiO<sub>2</sub>/SiO<sub>2</sub> reflectors based on 3-, 6-, and 9-stacks. The increased number of stacks yielded the maximum reflectance and resulted in the broadening of the reflection windows. In summary, the maximum reflectance was attained within the UV band at center wavelengths of 335 nm, 358 nm, and 367 nm corresponding to the 3-, 6-, and 9- stacks based reflectors. These reflectors are capable of prohibiting the propagation of a broad range of ultraviolet light, and therefore, they are promising as the UV protection coating of glass windows. Further, such reflectors are also beneficial in light-emitting diodes to maximize optical efficiency.

#### ACKNOWLEDGMENTS

This research grant was supported by the UGC-DAE Consortium for Scientific Research (Indore) under the collaborative research scheme.

#### References

- Abou-Helal M.O., Seeber W.T. (2002).** Preparation of TiO<sub>2</sub> thin films by spray pyrolysis to be used as a photocatalyst, *Appl. Surf. Sci.* 195(1-4), 53-62.
- Chalam, K.V. (2011).** Role of Ultraviolet Radiation in Age-Related Macular Degeneration, *Eye contact lens.* 37(4), 225-232.
- Dai, J. (2016).** Design and fabrication of UV band-pass filters based on SiO<sub>2</sub>/Si<sub>3</sub>N<sub>4</sub> dielectric distributed Bragg reflectors, *Appl. Surf. Sci.* 64, 886-891.

**Dubey, R.S. & Ganesan V. (2017).** Fabrication and Characterization of TiO<sub>2</sub>/SiO<sub>2</sub> based Bragg Reflectors for Light Trapping Applications, *Results Phys.* **7**, 2271-2276.

**Flannery, M. (1979).** Nearly perfect multilayer dielectric reflectors: theory, *Appl. Opt.* **18**(9), 1428-1435.

**Jung, S.C. (2008).** Photocatalytic activities and specific surface area of TiO<sub>2</sub> films prepared by CVD and sol-gel method, *Korean J. Chem. Eng.* **25**(2), 364-367.

**Kitano, M., Funatsu, K., Matsuoka, M., Ueshima, M., & Anpo, M. (2006).** Preparation of nitrogen substituted TiO<sub>2</sub> thin film photocatalysts by the radio frequency magnetron sputtering deposition method and their photocatalytic reactivity under visible light irradiation, *J. Phys. Chem. B.* **110**(50), 25266-25272.

**Lin, NM., Shei, SC., & Chang, SJ. (2015).** Design and Fabrication of a TiO<sub>2</sub>/SiO<sub>2</sub> Dielectric Broadband and Wide-Angle Reflector and Its Application to GaN-Based Blue LEDs, *IEEE J. Quantum Elect.* **51** (7), 1-5.

**Malherbe, A. (1974).** Interference filters for the far ultraviolet, *Appl. Opt.* **13**, 1275-1276.

**Monroy, E., Omnes, F., & Calle (2003).** Wide-bandgap semiconductor ultraviolet photodetectors, *Semiconduct. Sci. Technol.* **18**(4), R33-R51.

**Singh, D.P., Seung Hee Lee, II Yong Choi, & Jong Kyu Kim. (2015).** Spatially graded TiO<sub>2</sub>-SiO<sub>2</sub> Bragg reflector with rainbow-colored photonic bandgap, *Opt. Express.* **23**(13), 17568-17575.

**Spiller, E. (1974).** Interference filters for the ultraviolet and the surface plasmon of aluminum, *Appl. Opt.* **13**(6), 1209-1215.

**Subramanian, M., Vijayalakshmi, S., Venkataraj, S., & Jayavel, R. (2008).** Effect of cobalt doping on the structural and optical properties of TiO<sub>2</sub> films prepared by sol-gel process, *Thin Solid Films.* **516** (12), 3776-3782.

**Torchio, P., Gatto, A., Alvisi, M., Albrand, G., Kaise, N., & Amra. C. (2002).** High-reflectivity HfO<sub>2</sub>/SiO<sub>2</sub> ultraviolet mirrors, *Appl. Opt.* **41**(16), 3256-3261.

**Venkatesh Yepuri, Dubey, R. S. & Brijesh Kumar. (2020).** Fabrication and characterization of spectrally selective glazing dielectric multilayer structures, *Nanosystems: Phys. Chem. Math.* **11** (4), 488-492.

**Venkatesh Yepuri, Dubey, R. S., & Brijesh Kumar. (2020).** Rapid and economic fabrication approach of dielectric reflectors for energy harvesting applications, *Sci. Rep.* **10**, 1-9.

**Vincent, A., Babu, S., Brinley, E., Karakoti, A., Deshpande, & Seal, S. (2007).** Role of catalyst on refractive index tunability of porous silica antireflective coatings by sol-gel technique, *J. Phys. Chem. C.* **111**(23), 8291-8298.

**Wang, X., Chen, B., & Yao, L. (2018).** Design and Fabrication of Far-Ultraviolet Reflective Broadband Filter Based on Dielectric Materials, *J. Appl. Spectrosc.* **72**(6), 943-946.

**Wu, G., Wang, J., Shen, J., Yang, T., Zhang, Q., Zhou, B., Deng, Z., Fan, B., Zhou, D., & Zhang, F. (2001).** A new method to control nano-porous structure of sol-gel-derived silica films and their properties, *Mater. Res. Bull.* **36**(12), 2127-2139.



**Xie, Z.L., Zhang, R., Xiu, X.Q., Han, P., Liu, B., Chen, L., Yu, H.Q., Jiang, R.L., Shi, Y., & Zheng Y.D. (2007).** MOCVD growth and characteristics of high-quality AlGa<sub>N</sub> used in the DBR structure of ultraviolet detector, *Acta Phys. Sin. Chem. Ed.* 56(11), 6717-6721.

**Yonemaru, M., Kikuchi, A., & Kishino, K. (2002).** Improved Responsivity of AlGa<sub>N</sub>-Based Resonant Cavity-Enhanced UV Photodetectors Grown on Sapphire by RF-MBE, *Phys. stat. sol. (a)*. 192(2), 292-295.

**Yuehui, W., & Xing, Y. (2018).** High-reflection optical thin films based on SiO<sub>2</sub>/TiO<sub>2</sub> nanoparticles multilayers by dip coating, *Micro Nano Lett.* 13(9), 1349-1351.

**Zhang, Y., Gao, F., Gao, L., Hou, L., & Jia, Y. (2012).** Study of tri-layer antireflection coatings prepared by sol-gel method, *J. Sol-Gel Sci. Technol.* 62, 134-139.

**Zukic, M., & Torr, G. (1991).** Multiple reflectors as narrow-band and broadband vacuum ultraviolet filters, *Appl. Opt.* 31(10), 1588-1596.

**Submitted:** 07/10/2021

**Revised:** 07/11/2021

**Accepted:** 30/11/2021

**DOI:** 10.48129/kjs.16633